

Biochemical Analysis of the 20 S Proteasome of *Trypanosoma brucei**

Received for publication, January 8, 2003, and in revised form, February 21, 2003
Published, JBC Papers in Press, February 24, 2003, DOI 10.1074/jbc.M300195200

Ching C. Wang^{‡§}, Zbynek Bozdech[‡], Chao-lin Liu[‡], Aaron Shipway[¶], Bradley J. Backes[¶],
Jennifer L. Harris[¶], and Matthew Bogyo[¶]

From the Departments of [‡]Pharmaceutical Chemistry and [¶]Biochemistry and Biophysics, University of California, San Francisco, California 94143-0446 and the [¶]Department of Chemistry, Genomics Institute of the Novartis Research Foundation, San Diego, California 92121

We describe here biochemical characterization of the 20 S proteasome from the parasitic protozoan *Trypanosoma brucei*. Similar to the mammalian proteasome, the *T. brucei* proteasome is made up of seven α - and seven β -subunits. Of the seven β -type subunits, five contain pro-sequences that are proteolytically removed during assembly, and three of them are predicted to be catalytic based on primary sequence. Affinity labeling studies revealed that, unlike the mammalian proteasome where three β -subunits were labeled by the affinity reagents, only two β -subunits of the *T. brucei* proteasome were labeled in the complex. These two subunits corresponded to $\beta 2$ and $\beta 5$ subunits responsible for the trypsin-like and chymotrypsin-like proteolytic activities, respectively. Screening of a library of 137,180 tetrapeptide fluorogenic substrates against the *T. brucei* 20 S proteasome confirmed the nominal $\beta 1$ -subunit (caspase-like or PGPH) activity and identified an overall substrate preference for hydrophobic residues at the P1 to P4 positions in a substrate. This overall stringency is relaxed in the 11 S regulator (PA26)-20 S proteasome complex, which shows both appreciable activities for cleavage after acidic amino acids and a broadened activity for cleavage after basic amino acids. The 20 S proteasome from *T. brucei* also shows appreciable activity for cleavage after P1-Gln that is minimally observed in the human counterpart. These results demonstrate the importance of substrate sequence specificity of the *T. brucei* proteasome and highlight its biochemical divergence from the human enzyme.

barrel-shaped structure made up of a stack of four rings of proteins, each containing seven distinct protein subunits. The inner two rings contain β -type subunits, whereas the outer two rings contain α -type subunits (1, 3, 4). The α rings play mainly a structural role and have been shown to be important initiators of proteasome assembly (5). The primary proteolytic chamber of the CP contains six active sites resulting from three catalytically active subunits in each of the two inner β rings (6). Entry of substrate into the catalytic chamber is assisted by binding of a 19 S regulatory “cap” complex at the top and bottom of the 20 S CP (1, 2). This regulatory complex contains six ATPase subunits and 11 non-ATPase subunits and is required for the ATP-dependent degradation of ubiquitinated proteins (2, 7, 8). Additionally, substrate-binding properties of the CP can be altered by binding of an 11 S regulator complex, resulting in enhanced proteolytic activity and production of extended peptide substrate required for major histocompatibility complex class I-mediated antigen presentation (9–11). The human 11 S regulator protein has also recently been shown to alter the cleavage pattern and substrate specificity of the CP (12).

Eukaryotic proteasomes possess multiple peptidase activities that are classified into three major categories based upon the primary amino acid residues found at the site of hydrolysis. The “chymotrypsin-like” activity cleaves substrates after hydrophobic residues and is thought to be the primary activity of the complex required for initial attack on protein substrates. The “trypsin-like” activity cleaves substrates after basic residues and the “peptidyl-glutamyl peptide hydrolytic” (PGPH) or “caspase-like” activity cleaves after acidic residues (13, 14). These primary hydrolytic activities have been linked through mutagenesis and inhibitor studies to three catalytically active β subunits: $\beta 1$, $\beta 2$, and $\beta 5$ (15). These studies have assigned the chymotryptic activity to $\beta 5$, the tryptic activity to $\beta 2$, and the PGPH activity to $\beta 1$ (16). Hydrolysis by the proteasome is catalyzed by activation of a bound water molecule by the free N-terminal threonine residue found on all catalytically active β subunits (17). These N-terminal threonine residues are generated by proteolytic cleavage of extended precursor proteins during proteasome assembly, which serves as the primary mechanism to prevent pre-mature activation of incompletely assembled complexes (18). In addition, a lysine residue at position 33 of the mature β -subunit protein is essential for catalysis (19, 20).

Although the primary protease activities of the proteasome have been classified based on the amino acid residues found at the site of amide bond hydrolysis (P1 position), extensive in-

Proteasomes are multisubunit protein complexes responsible for the programmed degradation of protein substrates involved in a number of diverse cellular processes, including cell cycle progression, transcriptional regulation, and antigen presentation by major histocompatibility complex class I molecules (1, 2). The 20 S proteasome core particle (CP)¹ in eukaryotes is a

* This work was supported by National Institutes of Health Grant AI-21786. The costs of publication of this article were defrayed in part by the payment of page charges. This article must therefore be hereby marked “advertisement” in accordance with 18 U.S.C. Section 1734 solely to indicate this fact.

The nucleotide sequence(s) reported in this paper has been submitted to the GenBank™/EBI Data Bank with accession number(s) AF198386, AF148125, AF198387, AF169652, AF140353, AJ131148, AF169651, AJ131043, AJ130820, AF169653, AF226673, AF226674, AF148124, and AF290945.

§ To whom correspondence should be addressed. Tel.: 415-476-1321; Fax: 415-476-3382; E-mail: ccwang@cgl.ucsf.edu.

¹ The abbreviations used are: CP, core particle; VS, vinyl sulfone; NP, 4-hydroxy-3-nitrophenol; MAC, 4-methyl-7-aminocoumarin; PGPH,

peptidyl-glutamyl peptide hydrolytic; RFU, relative fluorescence unit(s); acc, 7-amino-4-carbamoylcoumarin; n and Nle, norleucine.

hibitor (21), substrate (22), and structural (23) studies have confirmed the importance of extended substrate recognition by the proteasome. In particular, variations at the P4 position of a substrate or inhibitor have a profound effect on recognition by individual β subunits (21, 22). Furthermore, recent observations suggested that the primary proteolytic activities of the mammalian proteasome might be linked through allosteric interactions in a bite-chew model (24). However, it is not yet clear if this substrate-induced regulation of hydrolysis may in fact result from multiple substrate binding sites on a single catalytic subunit.

Trypanosoma brucei is a parasitic protozoan that is the causative agent of African sleeping sickness. Resistance to commonly used anti-trypanosomal chemotherapeutics presents a potentially serious problem for most parts of sub-Saharan Africa (25, 26). Several unique characteristics of proteasome-mediated protein degradation in *T. brucei* have been recently reported. First, mouse ornithine decarboxylase expressed in *T. brucei* together with a rat antizyme was found to be highly stable (27), whereas this same protein complex is rapidly degraded by the 26 S proteasome in mammalian cells (28). Second, down-regulation of expression of each of the 7 α -subunits, 7 β -subunits, the 6 ATPase subunits, and the 11 non-ATPase subunits of the 26 S proteasome by RNA interference in *T. brucei* leads to intracellular accumulation of ubiquitinated proteins and blocked cell growth (29, 30). Third, the 11 S regulator PA26–20 S proteasome complex constitutes the predominant complex in *T. brucei* (31), yet a down-regulation of PA26 expression by RNA interference results in no detectable phenotype in the insect form of *T. brucei* (29). Thus, it is not clear how the various forms of proteasome in *T. brucei* are regulated for coordinated protein degradation, cell cycle progression, and development of *T. brucei*. A detailed biochemical analysis of the proteasome from *T. brucei* may help to explain how this enzyme complex differs from the human homolog. Such information is likely to help find ways to specifically target this essential cellular component of protein breakdown for therapeutic gain.

In the present study, we describe the subunit composition and biochemical properties of the *T. brucei* proteasome. Surprisingly, although five of the seven β -subunits undergo apparent post-translational modifications via proteolytic removal of a portion of the N termini, only two show proteolytic activity as measured by labeling with irreversible inhibitors. The profile of peptidase activities in the *T. brucei* 20 S proteasome suggests a stringent substrate specificity for the $\beta 1$ and the $\beta 2$ subunit and a broad substrate specificity for the $\beta 5$ subunit. These profiles became considerably less selective and included an increase in the caspase-like activity when the PA26 heptamer rings bound the 20 S CP, suggesting an 11 S regulator-induced structure-function change of the β -subunits. Comparison of overall substrate specificity of the *T. brucei* and human proteasome suggests that subtle differences exist that may aid in the design of specific inhibitors of this essential protease complex in trypanosome.

MATERIALS AND METHODS

***T. brucei* Cultures and 20 S Proteasome Purification**—*T. brucei* 427 strain procyclic form cells were cultured in Cunningham's medium supplemented with heat-inactivated fetal calf serum at a final concentration of 10% (32). Purification of the 20 S proteasome from *T. brucei* procyclic form cells was carried out as previously described (33). The human 20 S proteasome, purified from outdated human blood by previously described methods (34), was a kind gift from Prof. Martin Rechsteiner of the University of Utah.

Subunit N-terminal Sequence Determination—Two-dimensional protein gel analysis of the purified *T. brucei* 20 S proteasome was carried out as previously described (31). The separated subunit proteins in the gel were stained with Coomassie Blue, and each protein spot was

subjected to Edman degradations for N-terminal sequence determination at the Protein Core Facility, Howard Hughes Medical Institute, Columbia University, College of Physicians and Surgeons, New York, NY.

Competition Assay of Fluorogenic Substrate Hydrolysis—4-Hydroxy-3-nitrophenyl-Leu-Leu-Leu-vinylsulfone (NP-L₃-VS), Tyr-Leu-Leu-Leu-vinylsulfone (YL₃-VS), and 4-hydroxy-3-nitrophenol-Leu-Leu-Asn-vinylsulfone (NP-L₂N-VS) were synthesized and iodinated with ¹²⁵I as described (21, 35). Leupeptin (acetyl-Leu-Leu-DL-Arginal) was purchased from Boehringer Mannheim. Fluorogenic peptides succinyl-Leu-Leu-Val-Tyr-4-methyl-7-aminocoumarin Suc-(LLVY-MAC) and Gly-Gly-Arg-4-methyl-7-aminocoumarin (GGR-MAC) were purchased from Sigma. For peptidase assay, 1 μ g of the purified 20 S proteasome from *T. brucei* was suspended in 100 μ l of the peptidase assay buffer; 30 mM Tris-HCl, pH 7.8, 5 mM MgCl₂, 10 mM KCl, 0.5 mM dithiothreitol. Individual vinylsulfone derivatives or leupeptin were each added to the proteasome-containing peptidase assay buffer at varying concentrations and incubated at 25 °C for 45 min prior to adding 1 μ l of a 5 mM stock solution of fluorogenic peptide substrate. The assay mixture was further incubated at 25 °C for 60 min, and the enzyme-catalyzed reaction was stopped by 100 μ l of 2% SDS. The fluorescence in the mixture was measured with a fluorometer at an excitation wavelength of 360 nm and an emission wavelength of 460 nm.

Labeling of 20 S Proteasome with Iodinated Peptide Vinylsulfones—Purified *T. brucei* 20 S proteasome (1–3 μ g) was suspended in 100 μ l of TSDG (10 mM Tris-HCl, pH 7.4, 25 mM KCl, 10 mM NaCl, 1 mM MgCl₂, 0.2 mM EDTA, 1 mM dithiothreitol, 20% glycerol). ¹²⁵I-YL₃-VS, ¹²⁵I-NP-L₃-VS, and ¹²⁵I-NP-L₂N-VS were each added at 1.8×10^4 Bq/ml. The labeling reaction was carried out at 25 °C for 60 min and then stopped by adding 25 μ l of 5 \times Laemmli SDS-PAGE sample buffer to the reaction mixture (21). For competition experiments, 1–3 μ g of the purified *T. brucei* 20 S proteasome was preincubated with the unlabeled inhibitors (as indicated) under the identical conditions as for the labeling experiment. ¹²⁵I-YL₃-VS was then added to the reaction mixture at 1.8×10^4 Bq/ml. Protein labeling proceeded at 25 °C for 60 min and was then stopped by adding 25 μ l of 5 \times SDS sample buffer as before. The radiolabeled protein was fractionated and analyzed by 12% SDS-PAGE and autoradiography.

Substrate Library Kinetic Screening—The purified recombinant *T. brucei* 11 S regulator protein PA26 was prepared as previously described (31). Purified *T. brucei* 20 S proteasome (24 nM for assays without PA26, 2.4 nM for assays with 640 nM PA26) in a buffer containing 60 mM Tris-HCl, pH 7.5, 10 mM KCl, and 5 mM MgCl₂ was preincubated at 37 °C for 10 min to allow for association of the 20 S proteasome with PA26. The preincubated proteasome was then added to the substrate libraries, which were synthesized using methods described previously (22). The substrate concentration was 15 nM/substrate/well in the one-position fixed library at 6859 substrates/well (Cys was excluded and Met was replaced by the isosteric non-natural amino acid norleucine (Nle)). In the two-position fixed library, the substrate concentration was 0.25 μ M/substrate/well at 361 substrates/well (Cys was excluded and Met was replaced by Nle). Fluorescence was monitored for 30 min at λ_{ex} of 380 nm and λ_{em} of 450 nm in a Molecular Devices Gemini XS microtiter plate reader. The purified human 20 S proteasome was used to screen the substrate libraries by the same procedures (22).

Single Substrate Kinetics of the Human and *T. brucei* Proteasome—The following substrate sequences were designed to be selective substrates for the $\beta 1$, $\beta 2$, and $\beta 5$ subunits for both the human and the *T. brucei* proteasome: acetyl-EPPD-7-amino-4-carbamoylcoumarin (acc), acetyl-norleucine(n)RnR-acc, and acetyl-HHSL-acc. An additional substrate was designed based on the substrate specificity for cleavage after P1-Gln observed in the *T. brucei* proteasome, acetyl-YWTQ-acc. The purified 20 S proteasomes from human and *T. brucei* at a concentration of 20 nM were preincubated for 10 min in the assay buffer containing, 60 mM Tris-HCl, pH 7.5, 10 mM KCl, and 5 mM MgCl₂. Substrates were added at multiple concentrations, from 0.00001 to 1.75 mM (depending on solubility) to the preincubated enzyme, and substrate hydrolysis was monitored for 90 min at λ_{ex} of 380 nm and λ_{em} of 450 nm in a Molecular Devices Gemini XS microtiter plate reader. Data were fit using non-linear regression to the Michaelis-Menten equation and values for k_{cat} , K_m , and k_{cat}/K_m were determined.

RESULTS

Analysis of Biochemical Properties of the Subunits of *T. brucei* 20 S Proteasome—Samples of purified *T. brucei* 20 S proteasome were resolved by two-dimensional gel electrophoresis

TABLE I

Comparison of calculated molecular weights with those experimentally estimated molecular masses among *T. brucei* 20 S proteasomal subunits

Name	Molecular weight, calculated from encoding cDNA	Molecular mass, estimated from 2-D gel	Molecular weight, calculated from N-terminal determination
		<i>kDa</i>	
α 1	29333.76	28.0	
α 2	25352.94	24.3	
α 3	32175.98	33.0	
α 4	27863.44	27.0	27863.44
α 5	27174.86	27.5	
α 6	29333.00	29.0	
α 7	25460.94	25.0	
β 1	30439.31	24.7	24632.09
β 2	27400.50	24.0	24104.96
β 3	22456.31	23.2	22456.31
β 4	22756.50	23.8	
β 5	27965.95	22.7	22707.13
β 6	28713.67	24.5	24155.84
β 7	24407.27	24.0	24003.84

and stained with Coomassie Blue (data not shown). The identity of each protein spot on the stained gel was previously determined by mass spectrometric analysis (31). The molecular masses and pI values of each of the identified subunit proteins were estimated by their positions in the two-dimensional gel. These values were compared with the molecular weight and isoelectric point (pI) of each of the α - and the β -subunits of *T. brucei* 20 S proteasome calculated based on sequences of the full-length cDNAs encoding each protein (see footnote 2 and Tables I and II).²

Among the α -subunits, there is little discrepancy between the calculated molecular weights and the experimentally estimated molecular masses and only minor differences between the calculated and experimentally determined pI values for all subunits except α 1 (Tables I and II). This subunit has a calculated pI of 9.24 but an experimentally determined pI of 6.1. The molecular basis for this discrepancy remains unclear. On the other hand, five of the seven β -subunits demonstrated significantly lower molecular masses by two-dimensional gel when compared with their calculated molecular weights from the encoding cDNAs (Table I). These subunits, β 1, β 2, β 5, β 6, and β 7, also showed significant differences between their calculated and experimental pI values (Table II).

N-terminal sequence analysis of each of the 14 identified protein spots indicated that all the α -subunits with the exception of α 3 have blocked N termini. The experimentally determined N-terminal sequence of α 3 was identical to that of the predicted sequence, indicating no post-translational modification at its N terminus. Despite having blocked N termini, the α 2, α 4, α 5, α 6, and α 7 subunits had very similar predicted and measured molecular weights and pI values, suggesting a lack of significant modification of their N termini. However, a major post-translational modification of α 1 may have occurred, resulting in a blocked N terminus, a decreased molecular mass, and a dramatic decrease in its pI value (from 9.24 to 6.1). The precise structural changes involved in this post-translational modification remain to be elucidated.

Among the β -subunits, only β 4 was found blocked at its N terminus. This N-terminal modification does not result in a major change in either its molecular weight or its pI (Tables I

TABLE II

Comparison of calculated pI values with those experimentally estimated values among *T. brucei* 20 S proteasomal subunits

Name	pI		
	Calculated from encoding cDNA	Estimated from 2-D gel	Calculated from N-terminal determination
α 1	9.24	6.10	
α 2	5.95	5.90	
α 3	5.14	5.40	
α 4	6.64	6.40	6.64
α 5	4.71	4.50	
α 6	5.17	5.30	
α 7	5.37	5.20	
β 1	6.51	8.60	8.59
β 2	8.64	8.10	8.20
β 3	4.89	4.70	4.89
β 4	6.07	6.10	
β 5	8.90	7.50	7.38
β 6	6.56	6.00	6.08
β 7	5.96	5.80	5.96

and II). Sequencing of β 3 indicated that its N terminus matched that predicted by the encoding cDNA, whereas the remaining five β -subunits each lost a portion of their N termini (Fig. 1). N-terminal sequencing of these subunits identified N-terminal truncation of 53 residues from β 1, 29 residues from β 2, 46 residues from β 5, 41 residues from β 6, and 5 residues from β 7. The molecular weights and pI values derived from the corresponding truncated cDNAs agree well with those observed from the two-dimensional gel (Tables I and II). Among the five truncated β -subunits, β 1 and β 2 have an N-terminal amino acid sequence of TTI, whereas β 5 has the sequence TTTL, both of which are typical of the N termini of catalytically active β -subunits (19, 20). Furthermore, there is a conserved catalytic lysine residue at position 33 of each of these three matured β proteins (Fig. 2). The mature β 6 and β 7 subunits, on the other hand, lack both the catalytic Thr-1 and Lys-33 residues (Fig. 2), thus suggesting that β 1, β 2, and β 5 are the only catalytically active subunits of the *T. brucei* 20 S proteasome.

Active Site Labeling of the *T. brucei* 20 S Proteasome β -Subunits—Peptide vinylsulfone derivatives have been shown to function as irreversible inhibitors of the three primary peptidase activities of the mammalian and yeast 20 S proteasomes (21). These small molecule inhibitors act by formation of a covalent bond with the catalytic Thr-1 hydroxyl residues in each of the active β subunits. Because inhibition results in permanent modification of the active subunits, the radiolabeled version of these compounds can be used for biochemical analysis of each of the proteasome active sites. The peptide vinylsulfones, ¹²⁵I-NP-L₃-VS and ¹²⁵I-YL₃-VS, can be used to label the β 1, β 2, and β 5 as well as the γ -interferon-inducible subunits β 1i (LMP-2), β 2i (MECL-1), and β 5i (LMP-7) of the human 20 S proteasome (21). However, these compounds label the active sites with different relative intensities based on binding affinity, with YL₃-VS having a dramatically increased activity for the β 2 and β 2i subunits (21).

Labeling of purified *T. brucei* 20 S proteasome with ¹²⁵I-YL₃-VS revealed modification of only two subunits of apparent molecular masses of 22.7 and 24.0 kDa (Fig. 2). The identity of these two subunits was confirmed as the β 5 and the β 2 subunits, respectively, by mapping of the labeled proteins by two-dimensional gel electrophoresis (data not shown). Surprisingly, this radiolabeled vinylsulfone failed to label the *T. brucei* β 1 subunit (24.7 kDa), predicted to be catalytically active based on primary sequence and homology to the mammalian β 1 subunit. This result suggests that the β 1 either has a dramatically altered substrate specificity compared with the mammalian 20 S proteasome and is not sensitive to labeling or it is catalytically inactive. Interestingly, even upon addition of the PA26

² The GenBank™ database accession numbers of the DNA sequences encoding the 14 subunits of *T. brucei* 20 S proteasome are as follows: α 1, AF198386; α 2, AF148125; α 3, AF198387; α 4, AF169652; α 5, AF140353; α 6, AJ131148; α 7, AF169651; β 1, AJ131043; β 2, AJ130820; β 3, AF169653; β 4, AF226673; β 5, AF226674; β 6, AF148124; and β 7, AF290945.

```

*
Ta- $\beta$           mn $\underline{g}$ tl $\underline{e}$ t $\underline{g}$ T $\underline{T}$ VGITLKD $\underline{A}$ VIMATERRVTMENFIMHKNGK $\underline{K}$ LF...
Tb- $\beta$ 1       -53...pqlseavsl $\underline{g}$ T $\underline{T}$ IMAVSYKDG $\underline{V}$ VLAADSRTSTGAYV $\underline{V}$ NRASN $\underline{K}$ LA...
Tb- $\beta$ 2       -29...lhpprtlkt $\underline{g}$ T $\underline{T}$ IVGVVFE $\underline{G}$ GVV $\underline{L}$ GDATRATEGSIVADK $\underline{R}$ CK $\underline{K}$ IH...
Tb- $\beta$ 5       -46...Svpkldm $\underline{k}$ kgT $\underline{T}$ TLGFHF $\underline{D}$ GGII $\underline{I}$ AVDSRASSG $\underline{Q}$ YISSQ $\underline{T}$ V $\underline{M}$ K $\underline{V}$ L...
Tb- $\beta$ 6       -41...lplr $\underline{q}$ gakghP $\underline{Q}$ HWS $\underline{P}$ Y $\underline{T}$ DNGGT $\underline{I}$ AAIAGSN $\underline{Y}$ V $\underline{V}$ LGDATRL $\underline{N}$ G $\underline{D}$ F...
Tb- $\beta$ 7       masggSVI $\underline{G}$ LKYNGG $\underline{V}$ LLASDTLLSYGS $\underline{L}$ AKWPNI $\underline{P}$ RIK $\underline{I}$ ...

```

FIG. 1. Sequence alignment of the N terminus of *T. acidophilum* proteasome β -subunit (Ta- β) with the N-terminal regions from the five truncated *T. brucei* β -subunits. The sequences removed from the proteins during maturation are in lowercase, whereas the N-terminal sequences of the matured proteins are in capital letters. Numbers to the left of the *T. brucei* sequences indicate numbers of truncated residues. Bold letters under an asterisk indicate the important residues Thr-1 and Lys-33, respectively.

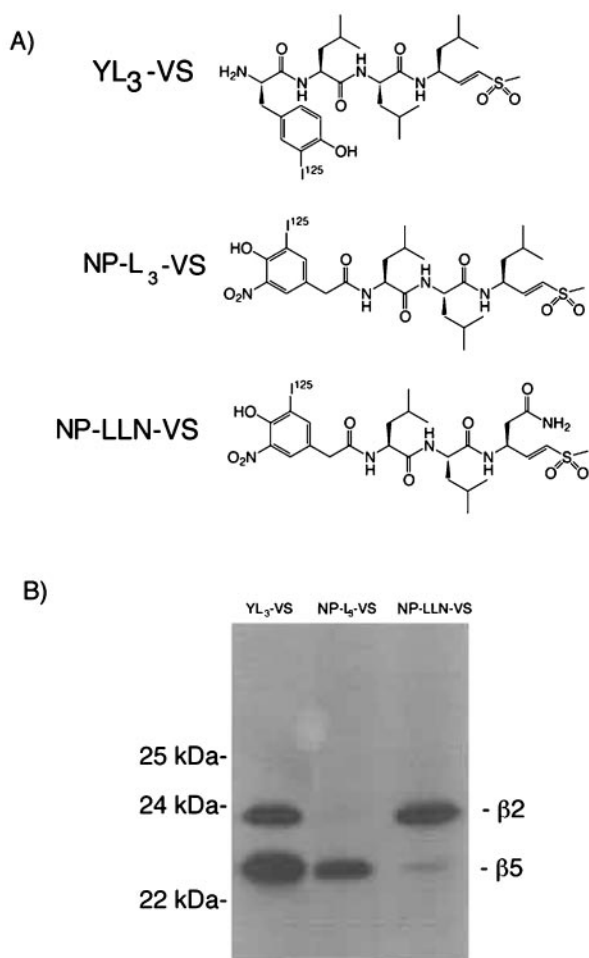


FIG. 2. Labeling of the catalytically active β -subunits in *T. brucei* 20 S proteasome with irreversible inhibitors. The ^{125}I -vinylsulfones used in the individual labeling experiments are indicated at the top of each lane.

cap complex to the 20 S core, the β 1 subunit still failed to label with the general affinity probe (data not shown).

Affinity labeling of the *T. brucei* proteasome with the related peptide vinylsulfone, ^{125}I -NP-L₃-VS resulted in modification of only the β 5 subunit, indicating an extended substrate specificity similar to that observed in the mammalian enzyme. Substitution of P1 Leu for Asn in ^{125}I -NP-L₃-VS results in an affinity probe, ^{125}I -NP-L₂N-VS, that labels almost exclusively the β 2 subunit of the *T. brucei* proteasome (Fig. 2). This strict substrate specificity differs from the human enzyme and suggests potentially divergent functional properties of *T. brucei* proteasome.

Inhibitor Specificity Profiles of the Primary Catalytic β -Subunits of the *T. brucei* Proteasome—The general probe ^{125}I -YL₃-VS can be used to assess the binding of other classes of

small molecule inhibitors to the proteasome active sites. To investigate the specificity in labeling β subunits of the *T. brucei* 20 S proteasome, YL₃-VS, NP-L₃-VS, NP-L₂N-VS, and leupeptin were each tested in competing with ^{125}I -YL₃-VS labeling of β 2 and β 5. As summarized in Fig. 3, NP-L₃-VS competes effectively only against labeling of β 5 ($\text{IC}_{50} = 7 \mu\text{M}$), whereas NP-L₂N-VS competes moderately only against labeling of β 2 ($\text{IC}_{50} = 22.5 \mu\text{M}$). These results are in perfect agreement with the labeling specificity profiles generated by direct labeling. Leupeptin, a specific inhibitor of the trypsin-like activity in mammalian 20 S proteasome (21), strongly inhibits the labeling of β 2 with a roughly estimated IC_{50} below $1 \mu\text{M}$ (Fig. 3) but with little effect on the labeling of β 5. Together these results suggest that the β 2 subunit possesses trypsin-like peptidase activity, whereas the β 5 subunit is responsible for the chymotrypsin-like peptidase activity.

Inhibition of Peptidase Activities of the *T. brucei* 20 S Proteasome—The *T. brucei* 20 S proteasome is capable of hydrolyzing a variety of short fluorogenic peptide substrates. Of the many commercial substrates tested, GGR-MAC was identified as the most efficient substrate (28) followed by Suc-LLVY-MAC as the next best substrate. Several other substrates such as IIW-MAC, PFR-MAC, and AAF-MAC underwent only limited hydrolysis (28), and no hydrolysis of AFK-MAC or YVAD-MAC was detectable. This limited substrate analysis suggests an unusual specificity profile favoring Arg and hydrophobic residues at the P1 position of a substrate. To investigate the potential contributions of β 2 and β 5 subunits to hydrolysis of the GGR-MAC and Suc-LLVY-MAC substrates, inhibition studies were performed with the same set of inhibitors used for the competition studies in Fig. 3. Hydrolysis of GGR-MAC was inhibited by each of the four inhibitors with estimated IC_{50} values of $48 \mu\text{M}$ for YL₃-VS, $40 \mu\text{M}$ for NP-L₃-VS, $63 \mu\text{M}$ for NP-L₂N-VS, and $1.5 \mu\text{M}$ for leupeptin and 33, 7, 77, and $>100 \mu\text{M}$, respectively, for the same inhibitors for hydrolysis of Suc-LLVY-MAC (data not shown). Leupeptin therefore is the most potent inhibitor of GGR-MAC hydrolysis and the most active competitor for labeling of β 2 (Fig. 3), indicating that the β 2 subunit catalyzes hydrolysis of the GGR-MAC substrate. Similarly, NP-L₃-VS is the most potent inhibitor of Suc-LLVY-MAC hydrolysis and labels only the β 5 subunit. It is likely responsible for hydrolysis of the Suc-LLVY-MAC substrate.

Substrate Specificity of *T. brucei* 20 S Proteasome and Its 11 S Regulator Complex—To further elaborate the substrate specificity of the *T. brucei* 20 S proteasome and to compare the profile to that of the human enzyme, kinetic screening was performed using a P1–P4 diverse, positionally scanned library of peptide substrates. Such libraries have been developed to sequentially analyze the specificity of proteolytic enzymes by measurement of kinetic constants for individual library members with a single fixed amino acid at a single position in the substrate. Library data can then be used to construct optimal peptide substrates that correlate with the optimal or specific primary sequences on protein substrate.

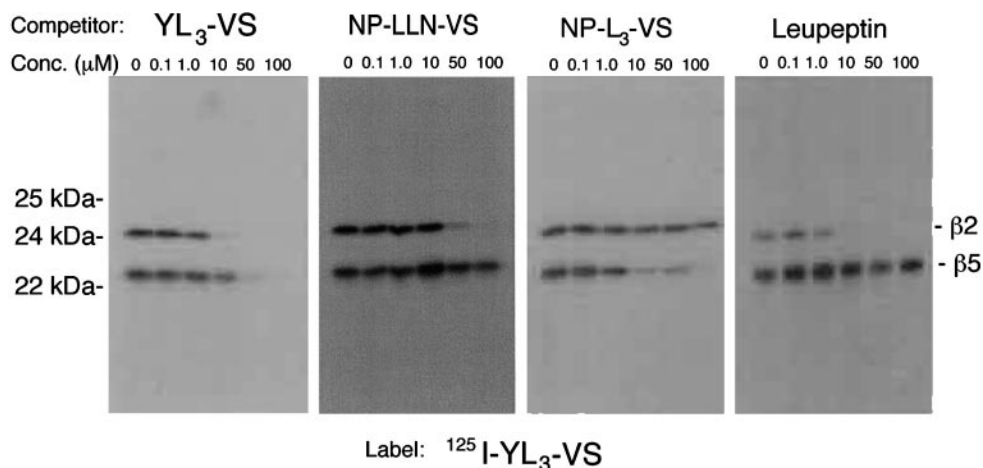


FIG. 3. Competition of unlabeled irreversible inhibitors with ^{125}I -YL₃-VS labeling of *T. brucei* 20 S proteasome. Identities of unlabeled competing inhibitors are presented above each panel with their concentrations stated (in micromolar) at the top of each lane in SDS-PAGE.

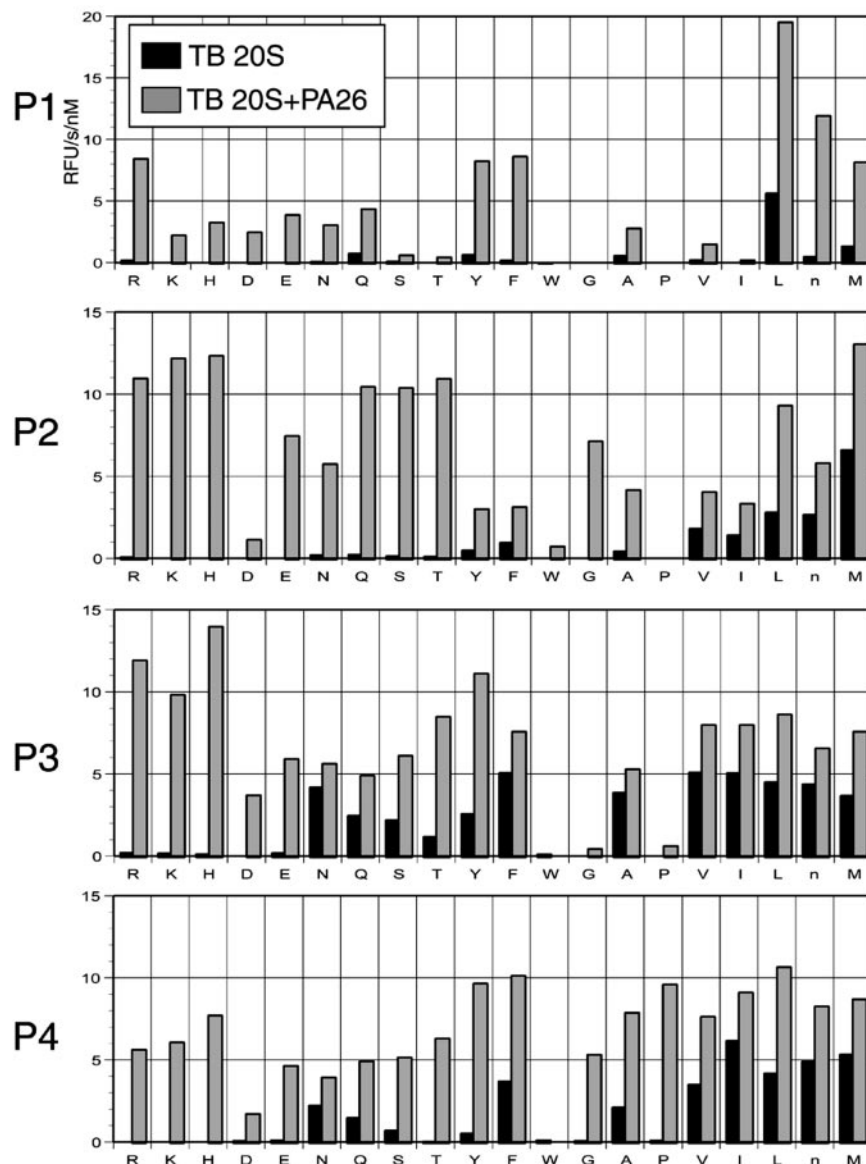


FIG. 4. Results from the one-position fixed scanning library where the y-axis represents the rate of substrate cleavage in relative fluorescence units over time per nM *T. brucei* 20 S proteasome (RFU/s/nM), and the x-axis represents the fixed amino acid. The *T. brucei* 20 S is shown by the black bars, and the *T. brucei* 20 S complexed to PA26 is shown by the gray bars.

Substrate scanning of the *T. brucei* 20 S proteasome indicates that the major activity of the complex is for cleavage after P1-leucine residues with additional minor activities prefer-

ring a P1-hydrophobic amino acid such as Met, Ala, Val, and Tyr and polar or basic amino acids Arg and Gln (see Figs. 4 and 6). In agreement with the labeling and inhibitor results,

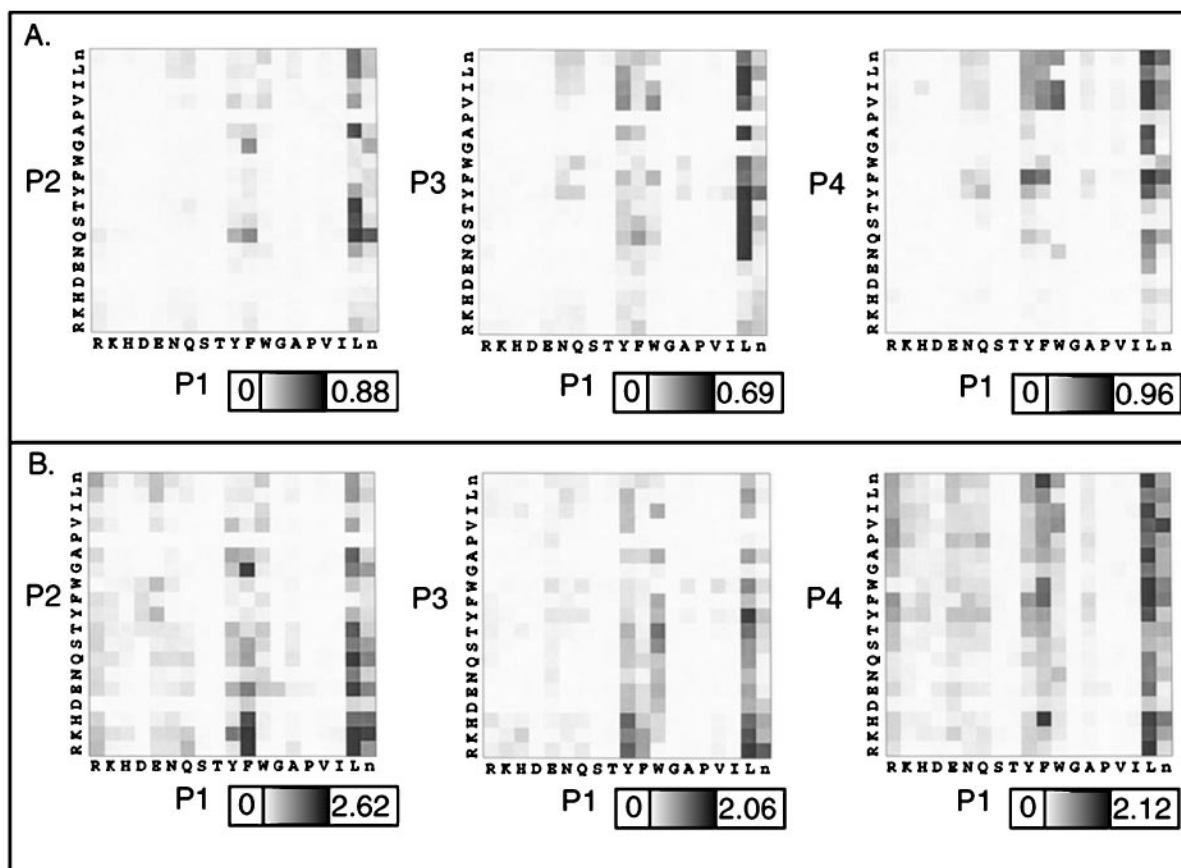


FIG. 5. Results from the two-position fixed libraries, where the *shade of the square* represents the RFU/s/nM and the x- and y-axes represent the P1-, P2-, P3-, P4-amino acid. A, *T. brucei* 20 S; B, *T. brucei* 20 S complexed to PA26.

there is little PGP activity detected in the one-position fixed library. *T. brucei* 20 S proteasome was also analyzed in the presence of the 11 S regulator. As anticipated, a dramatic increase in the existing peptidase activities was observed upon addition of the 11 S regulator complex (Fig. 4). In addition, the cleavage after P1-Glu, Asp, His, and Lys, which were undetectable in 20 S proteasome, were induced by formation of the 11 S-20 S proteasome complex (Fig. 4) suggesting broadening of substrate specificity as a result of the complex formation. A control experiment with the 11 S regulator alone showed negligible background activity.

Analysis of the extended substrate specificity (positions P2, P3, and P4) of the 20 S proteasome indicates that the preference at these sites is similar to that of P1 site, preferring aliphatic and hydrophobic amino acids (Fig. 4). A similar broadening of activity in the 11 S regulator-20 S proteasome complex to accept polar and charged amino acids was also observed for the extended P2, P3, and P4 positions regardless of the amino acid residue found at the P1 position (Fig. 4).

A comprehensive view of the interdependence for the P1 to P4 diversity space was assessed by employing a two-position fixed library for substrate analysis of both the core 20 S and the 11 S-20 S complexes (Fig. 5). Overall, the resulting activity profiles mirror those seen in the single fixed position library. The peptidase activity of 20 S proteasome is clustered in the hydrophobic region of substrate residues, again suggesting that hydrophobic amino acids at P1 to P4 facilitate peptide hydrolysis (Fig. 5A). The profile of the 11 S regulator-proteasome complex becomes considerably broader to include the acidic as well as the basic amino acids, and the importance of the extended binding sites up to P4 is demonstrated (Fig. 5B). Upon closer examination of the substrate specificity profiles, several

unique features of the individual peptidase activities emerge. For example, proline is tolerated at the P2 position, irrespective of the amino acid at P1. Conversely, a proline at the P3 position is only tolerated well if P1 is an acidic amino acid: aspartic acid or glutamic acid. Another notable feature of the dependences between sites that is observed by this data is the change in P2 and P3 selectivity for cleavage after large hydrophobic P1 amino acids upon 11 S cap binding. In the presence of the 11 S cap, the 20 S protease cleaves more efficiently substrate P1-hydrophobic amino acids with basic amino acids in the P2 and P3 positions, whereas in the absence of the 11 S cap, basic amino acids are clearly disfavored.

Finally, the profiles of *T. brucei* and human 20 S proteasomes resulting from screening against the one-position fixed library were compared (Fig. 6). The results indicate that, although the profiles of hydrophobic amino acids from P1 to P4 appear similar between the two, the human 20 S proteasome shows clear recognition of Glu, Asp, His, and Lys at these positions, whereas *T. brucei* 20 S proteasome does not. However, one distinguishing additional activity observed in the *T. brucei* proteasome over the human proteasome is for cleavage after glutamine (Fig. 6). To test the magnitude of these differences, single substrates were designed and Michaelis-Menten kinetics performed for both the *T. brucei* and the human 20 S proteasomes. The results show that the overall kinetics of substrates is less efficient for the *T. brucei* proteasome for cleavage of substrates with P1-Leu, P1-Asp, and P1-Arg, as observed by decreased k_{cat}/K_m (Table III). In contrast to this observation, the activity is dramatically increased for cleavage by the *T. brucei* proteasome for substrates with P1-glutamine as predicted from the substrate specificity libraries (Table III). These differences in activity may indicate differences in the

FIG. 6. Comparison of results from the one-position fixed libraries for the 20 S proteasome from *T. brucei* (black) and human (gray). The y-axis represents the normalized activity (RFU/s), and the x-axis represents the fixed amino acid.

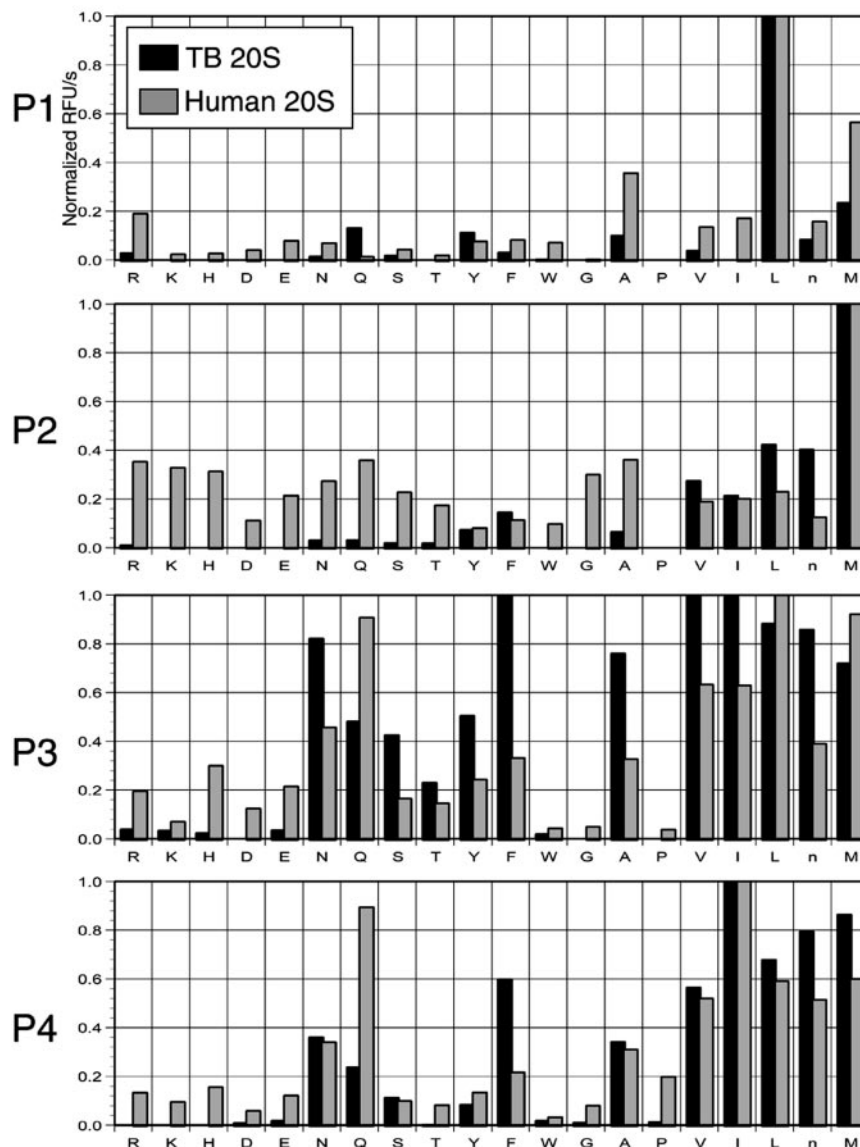


TABLE III
Kinetic constants of human 20 S proteasome and *T. brucei* proteasome against selected substrates

Substrate	Human 20 S proteasome			<i>T. brucei</i> 20 S proteasome			Ratio, $(k_{cat}/K_m)_{T. brucei} / (k_{cat}/K_m)_{human}$
	k_{cat} s^{-1}	K_m μM	k_{cat}/K_m $M^{-1}s^{-1}/10^4$	k_{cat} s^{-1}	K_m μM	k_{cat}/K_m $M^{-1}s^{-1}/10^4$	
Ac-HHSL-acc	36.30 ± 5.00	360 ± 160	9.85 ± 3.15	NS ^a	NS	0.45 ± 0.02	0.05
Ac-EPPD-acc	17.16 ± 0.39	32 ± 3	53.25 ± 3.25	2.70 ± 0.26	88 ± 19	3.11 ± 0.38	0.06
Ac-nRnR-acc ^b	5.34 ± 0.23	110 ± 14	5.06 ± 0.47	8.15 ± 1.55	670 ± 190	1.22 ± 0.12	0.24
Ac-YWTQ-acc	0.27 ± 0.04	27 ± 13	0.98 ± 0.29	4.67 ± 0.92	38 ± 17	12.04 ± 3.13	12.29

^a "NS" indicates that the enzyme was not saturated at the highest concentration tested (1.75 mM).

^b "n" in substrate Ac-nRnR-acc indicates norleucine.

active sites between the *T. brucei* and the human proteasomes that could be exploited for therapeutic intervention of trypanosomiasis. The potential significance of this difference will be discussed below.

DISCUSSION

In the present investigation, we perform detailed biochemical analysis of the *T. brucei* proteasome. Analysis of subunit composition of the complex indicated that five out of the seven β -subunits of *T. brucei* 20 S proteasome have N-terminal segments that are proteolytically processed during maturation. Among the five mature subunits, only β_1 , β_2 , and β_5 have Thr-Thr at their N termini and a Lys at position 33. Thus, they

likely represent the primary catalytically active subunits (19, 20). *Saccharomyces cerevisiae* and mammalian 20 S proteasomes undergo similar processing of these same five β -subunit precursors during assembly, and only β_1 , β_2 , and β_5 are catalytically active in the mature enzyme complexes (20, 36). It is yet unclear why the 20 S proteasome of *Thermoplasma acidophilum* (37) utilizes only a single chymotrypsin-like β -subunit and how this single subunit evolved to produce seven different β -subunits found in the eukaryotic 20 S proteasome. A close scrutiny of the β -subunits in *T. brucei* reveals that truncation of the 33 N-terminal residues from the β_3 subunit would result in a threonine at position 1 and a lysine at position 33.

Similarly, removal of the N-terminal 3 residues of $\beta 4$ subunit would result in a Thr-Thr-Ile sequence at the N terminus with a lysine at position 33. However, processing of these subunits does not occur by these predictions most likely due to the lack of a Gly residue directly N-terminal to the threonine at the site of hydrolysis. This Gly residue is highly conserved and is required for processing the $\beta 1$, $\beta 2$, and $\beta 5$ precursors (38) (Fig. 1). Interestingly, removal of the 53 N-terminal residues from the $\beta 6$ subunit would result in threonine at position 1 and a lysine at position 33. The required Gly residue directly N-terminal to the predicted Thr1 is also found in this subunit, yet the actual truncation takes place between His-41 and Pro-42, resulting in a catalytically inactive subunit. In the case of the $\beta 7$ subunit, removal of N-terminal five residues from the precursor occurs, resulting in a product with a serine at position 1 and a lysine at position 34 (Fig. 2). This mature protein is apparently enzymatically inactive even though serine has been shown to function in place of the catalytic threonine in mutant β subunits of the yeast proteasome (36).

These data support the conclusion that evolution of the seven originally identical β -subunits may have taken place, preventing some subunits from maturing to become active enzymes. Alternatively, some of the subunits may have lost their catalytic activity through accumulated random mutations. Only three β -subunits have retained the enzymatic activity with varied substrate specificities. Preservation of this set of three active β -subunits may be attributed to the three indispensable peptidase activities that are required of the proteasomes to carry out its necessary biological role in eukaryotes. It is therefore surprising that the $\beta 1$ subunit of the *T. brucei* 20 S proteasome has little PGPH activity. The trypsin-like $\beta 2$ subunit also demonstrates a limited profile of activity even though the basic P1 substrate GGR-MAC is an effective substrate (28). However, the dominant form of the proteasome in *T. brucei* is the 11 S regulator (PA26)-20 S proteasome complex (31), which has a full spectrum of enhanced and broad spectrum peptidase activities (Fig. 4). Surprisingly, down-regulated expression of PA26 does not affect the *in vitro* growth of the procyclic form of *T. brucei* (29), suggesting that other forms of the proteasome may exist that can compensate for the lack of 11 S regulator complexes.

Alignment of the sequences of *T. brucei* $\beta 1$ and $\beta 2$ with those from yeast and human fails to explain the lack of $\beta 1$ activity and the restricted $\beta 2$ activity in *T. brucei* 20 S proteasome. All of the catalytic subunits share considerable sequence identities from *T. brucei* to human with complete conservation of all pivotal active site residues (39). Most likely, additional structural requirements on the rest of protein backbone in *T. brucei* 20 S proteasome also play essential roles (40). This method of regulation is indirectly supported by the observations that the $\beta 1$ subunit becomes activated and $\beta 2$ substrate specificity is broadened upon addition of the 11 S regulator (PA26) complex (Figs. 4 and 5). Recently, the crystal structure of *T. brucei* 11 S regulator (PA26)-yeast 20 S proteasome complex was determined at 3.2-Å resolution (41). A major structural change is induced upon binding of the 11 S regulator to the yeast 20 S proteasome. This change results in widening of the opening of the proteasome from a diameter of 13 to 32 Å, which may be accompanied by multiple structural changes within the proteasomal channel that are not visible in this relatively low resolution structure. Similar structural changes in *T. brucei* 20 S proteasome induced by PA26 heptamer binding could bring about the observed functional activation in $\beta 1$ and specificity change in $\beta 2$.

Labeling of the proteolytically active β subunits of the *T. brucei* proteasome with covalent affinity probes showed a

unique profile that is significantly different from that of the mammalian 20 S proteasome (21). In particular, NP-L₃-VS can label human $\beta 2$ but not *T. brucei* $\beta 2$, whereas NP-L₂N-VS can label human $\beta 5$ but not *T. brucei* $\beta 5$. It appears that *T. brucei* β -subunits have an alternative substrate specificity comparing with the corresponding human β -subunits. This observation indicates that the *T. brucei* proteasome may have distinct functional properties that are reflected in its substrate specificity profiles. Furthermore, the labeling results indicate that residues positioned at P4 and P1 are both critical for directing substrates to the active subunits in *T. brucei* 20 S proteasome, as was recently shown for the human 20 S proteasome (12).

A similar finding was also made from a kinetic screen of *T. brucei* 20 S proteasome using one-position fixed fluorogenic substrate libraries (Fig. 4). The activity profiles for the P1, P2, P3, and P4 positions appear quite similarly oriented toward primarily hydrophobic residues, and P3 appears to have the most pronounced effect on substrate suitability. Similar results were also obtained for the human 20 S proteasome (Fig. 6). Comparison between the proteasome from human and *T. brucei* revealed several activities that appear to be specific to the *T. brucei* proteasome, namely cleavage after P1-glutamine substrates. Indeed, a single substrate designed with a glutamine at P1 showed a 12-fold increase in the activity of *T. brucei* proteasome versus the human proteasome. These differences in activities and specificities may be the initial step into elucidating the different structural requirements for the *T. brucei* proteasome and the human proteasome and open a window of opportunity for therapeutic drug design.

The results from both the inhibitor and substrate studies suggest a general rule that the amino acid in the P1 position alone does not determine the substrate specificity of the 20 S proteasome. Rather, it is the extended peptide sequence that dictates the specificity. Furthermore, the similar preference for hydrophobic residues among P1, P2, P3, and P4 positions suggests that it is the overall hydrophobic property of the peptide that makes a good substrate for the 20 S proteasome. The qualification for a good substrate may not only be determined by recognition of specific P1 residues among the individual β subunits but also by the ease of a substrate to enter the catalytic chamber of a 20 S proteasome, which may involve an initial interaction with the interior of an α -ring. In the case of *T. brucei* and human 20 S proteasomes, hydrophobic peptides may be more capable of entering the catalytic chamber to be digested.

The enhanced and broadened activity profiles exhibited by the 11 S regulator (PA26)-*T. brucei* 20 S proteasome complex indicate that, in addition to the hydrophobic amino acids, charged and polar amino acids, such as Glu, Asp, His, Lys, and Arg, at the P1, P2, P3, and P4 positions of the substrate are also capable of improving the kinetics of substrate digestion (Figs. 4 and 5). With the addition of the 11 S regulator (PA26), it appears that a more diverse subset of peptides is able to access to the catalytic chamber of the complex. This finding, coupled with the potential activation of $\beta 1$ and $\beta 2$ through structural changes inside the chamber (see above), could explain how the proteasome is regulated by addition of cap complexes to the 20 S core. The recently reported crystal structure of 11 S regulator (PA26)-yeast 20 S proteasome complex supports this mechanism (41). The seven activation loops in the interior of the PA26 heptamer ring are located around the chamber opening on top of the α -ring. These loops may play a pivotal role in facilitating entrance of ionic peptide into the catalytic chamber of proteasome. Further analysis through site-directed mutagenesis of PA26 may provide some answer to this postulation.

Overall, a fairly thorough structure-activity analysis of the

β -subunits in *T. brucei* 20 S proteasome was conducted. Their unique features, including the lack of β 1 activity and the restricted spectrum of β 2 activity, were found all "normalized" in *T. brucei* 11 S regulator (PA26)-20 S proteasome complex. An 11 S regulator-induced structural change of the proteasomal catalytic chamber was speculated to cause the functional change. However, in view of the apparent failure of the irreversible inhibitors in labeling the β 1 subunit in the 11 S regulator-20 S proteasome complex (preliminary data), we cannot yet rule out the possibility that acidic substrates could be degraded by β 2 and β 5 to some extent due to enhanced substrate accessibility to the catalytic chamber while β 1 remains still inactive. The subsequent finding that all residues from P1 to P4 of the substrate were important determining factors of the proteasomal activity profiles confirmed a previous similar observation in human proteasome (12) that the overall property of the peptide may be the major determinant of substrate suitability for proteasome. Most interestingly, the strong preference for substrate with glutamine at the P1 position by *T. brucei* proteasome has revealed a major discrepancy from the human proteasome. It may provide a rare opportunity for selective drug design against trypanosomiasis.

Acknowledgments—We are grateful to Professor Martin Rechsteiner of the University of Utah for the kind gift of purified human 20 S proteasome. We also thank Dr. Ziyin Li of the University of California at San Francisco for valuable assistance during the preparation of the manuscript.

REFERENCES

- Coux, O., Tanaka, K., and Goldberg, A. L. (1996) *Annu. Rev. Biochem.* **65**, 801–847
- Hochstrasser, M. (1996) *Annu. Rev. Genet.* **30**, 405–439
- Baumeister, W., Walz, J. K., Zuhl, F., and Seemuller, E. (1998) *Cell* **92**, 367–380
- Groll, M., Ditzel, L., Lowe, J., Stock, D., Bochtler, M., Bartunik, H. D., and Huber, R. (1997) *Nature* **386**, 463–471
- Yang, Y., Fruh, K., Ahn, K., and Peterson, P. A. (1995) *J. Biol. Chem.* **270**, 27687–27694
- Glickman, M. H., Rubin, D. M., Coux, O., Wefes, I., Pfeifer, G., Cjeka, Z., Baumeister, W., Fried, V. A., and Finley, D. (1998) *Cell* **94**, 615–623
- Glickman, M. H., Rubin, D. M., Fried, V. A., and Finley, D. (1998) *Mol. Cell. Biol.* **18**, 3149–3162
- Ciechanover, A. (1998) *EMBO J.* **17**, 7151–7160
- Preckel, T., Fung-Leung, W. P., Cai, Z., Vitiello, A., Salter-Cid, L., Winqvist, O., Wolfe, T. G., Von Herrath, M., Angulo, A., Ghazal, P., Lee, J. D., Fourie, A. M., Wu, Y., Pang, J., Ngo, K., Peterson, P. A., Fruh, K., and Yang, Y. (1999) *Science* **286**, 2162–2165
- Ahn, J. Y., Tanahashi, N., Akiyama, K., Hisamatsu, H., Noda, C., Tanaka, K., Chung, C. H., Shibmara, N., Willy, P. J., Mott, J. D., Slaughter, C. A., and DeMartino, G. N. (1995) *FEBS Lett.* **366**, 37–42
- Tanahashi, N., Yokota, K., Ahn, J. Y., Chung, C. H., Fujiwara, T., Takahashi, E., DeMartino, G. N., Slaughter, C. A., Toyonaga, T., Yamamura, K., Shimbara, N., and Tanaka, K. (1997) *Genes Cells* **2**, 195–211
- Nazif, T., and Bogyo, M. (2001) *Proc. Natl. Acad. Sci. U. S. A.* **98**, 2967–2972
- Orlowski, M. (1990) *Biochemistry* **29**, 10289–10297
- Rivett, A. J. (1989) *J. Biol. Chem.* **264**, 12215–12219
- Enenkel, C., Lehmann, H., Kipper, J., Guckel, R., Hilt, W., and Wolf, D. H. (1994) *FEBS Lett.* **341**, 193–196
- Arendt, C. S., and Hochstrasser, M. (1997) *Proc. Natl. Acad. Sci. U. S. A.* **94**, 7156–7161
- Brannigan, J. A., Dodson, G., Duggleby, H. J., Moody, P. C., Smith, J. L., Tomchick, D. R. and Murzin, A. G. (1995) *Nature* **378**, 416–419
- Zwickl, P., Kleinz, J., and Baumeister, W. (1994) *Nat. Struct. Biol.* **1**, 765–770
- Lowe, J., Stock, D., Jap, B., Zwickl, P., Baumeister, W., and Huber, R. (1995) *Science* **268**, 533–539
- Seemuller, E., Lupas, A., Stock, D., Lowe, J., Huber, R., and Baumeister, W. (1995) *Science* **268**, 579–582
- Bogyo, M., Shin, S. B., McMaster, J. S., and Ploegh, H. L. (1998) *Chem. Biol.* **5**, 307–320
- Harris, J. L., Alper, P. B., Li, J., Rechsteiner, M., and Backes, B. J. (2001) *Chem. Biol.* **8**, 1131–1141
- Groll, M., Nazif, T., Huber, R., and Bogyo, M. (2002) *Chem. Biol.* **9**, 655–662
- Kisselev, A. F., Akopian, T. N., Castillo, V., and Goldberg, A. L. (1999) *Mol. Cell* **4**, 395–402
- Borst, P., and Fairlamb, A. H. (1998) *Annu. Rev. Microbiol.* **52**, 745–778
- Maser, P., Sutterlin, C., Kralli, A., and Kaminsky, R. (1999) *Science* **285**, 242–244
- Bass, K. E., Sommer, J. M., Cheng, Q. L., and Wang, C. C. (1992) *J. Biol. Chem.* **267**, 11034–11037
- Hua, S. B., Li, X., Coffino, P., and Wang, C. C. (1995) *J. Biol. Chem.* **270**, 10264–10271
- Li, Z., Zou, C.-B., Yao, Y., Hoyt, M. A., McDonough, S., Mackey, Z. B., Coffino, P., and Wang, C. C. (2002) *J. Biol. Chem.* **277**, 15486–15498
- Li, Z., and Wang, C. C. (2002) *J. Biol. Chem.* **277**, 42686–42693
- Yao, Y., Huang, L., Krutchinsky, A., Wong, M. L., Standing, K. G., Burlingame, A. L., and Wang, C. C. (1999) *J. Biol. Chem.* **274**, 33921–33930
- Cunningham, I. (1977) *J. Protozool.* **24**, 325–329
- Hua, S., To, W. Y., Nguyen, T. T., Wong, M. L., and Wang, C. C. (1996) *Mol. Biochem. Parasitol.* **78**, 33–46
- Realini, C., Jensen, C. C., Zhang, Z., Johnston, S. C., Knowlton, J. R., Hill, C. P., and Rechsteiner, M. (1997) *J. Biol. Chem.* **272**, 25483–25492
- Bogyo, M., McMaster, J. S., Gaczynska, M., Tortorella, D., Goldberg, A. L., and Ploegh, H. (1997) *Proc. Natl. Acad. Sci. U. S. A.* **94**, 6629–6634
- Heinemeyer, W., Fischer, M., Krimmer, T., Stachon, U., and Wolf, D. H. (1997) *J. Biol. Chem.* **272**, 25200–25209
- Zwickl, P., Grziwa, A., Puhler, G., Dahlman, B., Lottspeich, F., and Baumeister, W. (1992) *Biochemistry* **31**, 964–972
- Chen, P., and Hochstrasser, M. (1996) *Cell* **86**, 961–972
- Huang, L., Shen, M., Chernushevich, I., Burlingame, A. L., Wang, C. C., and Robertson, C. D. (1999) *Mol. Biochem. Parasitol.* **102**, 211–223
- Groll, M., Hinemeyer, W., Jager, S., Ullrich, T., Bochtler, M., Wolf, D. H., and Huber, R. (1999) *Proc. Natl. Acad. Sci. U. S. A.* **96**, 10976–10983
- Whitby, F. G., Masters, E. I., Kramer, L., Knowlton, J. R., Yao, Y., Wang, C. C., and Hill, C. K. (2000) *Nature* **408**, 115–120